CARDIOVASCULAR SOLUTIONS

ZAN MITREV

2017

Co-Authors

Lidija Veljanovska-Kiridzievska, MD, Radiologist

Zvonko Atanasov, MD, Radiologist

Rodney Rosalia, PhD, Scientific Officer

Tanja Anguseva, MD, Interventional Cardiologist

Digital imaging editing

Daniel Veljanovski

Proofreading

www.Proof-Reading-Service.com

Devonshire Business Centre, Works Road,

Letchworth Garden City, SG6 1GJ,

Hertfordshire, United Kingdom

FOREWORD

Marko Turina, MD

Professor of surgery, University of Zurich, Switzerland

The present book, Cardiovascular Solutions, is a collection of clinical cases managed by Dr Zan Mitrev. Dr Mitrev is a surgeon with vast experience in the treatment of various cardiovascular pathologies, which he has meticulously documented in this book through numerous angiography analysis methods, guided by stunning pictures generated with CT angiography.

"Cardiovascular Solutions" is a unique collection of various cardiovascular, and related, diseases and the successful clinical management, using state-of-the-art surgical approaches, e.g. the hybrid technique of complex aortic arch pathologies.

Chapter 1 - The Heart, briefly introduces the reader to the cardiac vessels followed by several illustrations of coronary artery disease (CAD) and bypass grafting; the chapter represents a series of modern surgical techniques, e.g. arterial revascularization, the use of both internal mammary arteries and late follow-up of various surgical solutions.

Chapter 2 - Congenital Heart Diseases describes several cases of surgical approaches of congenital malformations in adults.

A substantial part of the book, **Chapter 3 - The Aorta**, deals with aortic diseases and their elegant surgical solutions, such as complex aortic dissections, reoperations and aortic ruptures. Carotid pathologies and their surgical solutions are the subjects of **Chapter 4 – The vertebrobasilar arteries and the Jugular vein**, which includes rare cases of glomus tumours, carotid aneurysms, cross-over grafts in the neck and vertebral revascularization. The diagnosis and treatment of peripheral vascular pathologies is the focus of **Chapter 5 - The Peripheral Blood Vessels**, and demonstrates the author's broad vascular surgical skills, experience and knowledge as well as an exceedingly rare attribute in the present "sub-specialisation in surgery".

I highly recommend Dr Mitrev's book to residents in cardiology or cardiovascular surgery, but also to undergraduate medical students wishing to expand their knowledge beyond their regular curriculum.

In summary, the excellent documentation of cardiovascular pathologies, combined with the various multidisciplinary interventions, provide a vivid picture of the possibilities of modern surgical treatment of cardiovascular pathologies.

PREFACE

Zan Mitrev

Hospital Director at the Special Hospital for Surgery Diseases
"Zan Mitrev Clinic", Skopje, Republic of Macedonia

I wrote this book to support all medical personnel working in the field of cardiovascular diseases, particularly staff engaged in the surgical management of cardiovascular pathologies.

I describe intriguing and rare cases from the everyday practice at the Zan Mitrev Clinic (previously the Special Hospital for Surgical Diseases "Filip Vtori") in Skopje, Macedonia. Arguably, the book portrays the development of cardiovascular surgery in the Republic of Macedonia since its conception in the early 2000s.

Through individual case reports, this book provides a comprehensive overview of advanced diagnostic and surgical therapeutic modalities of cardiovascular diseases. For instance, the evolution of simultaneous multislice imaging as well as of 3D reconstructions of the anatomy, physiology and tissue characteristics of the blood vessels has dramatically improved the success rate of cardiovascular surgeries.

This book intends to generate interest by abstaining from a large volume of text and by presenting a large number of images obtained via the application of advanced radiological, echocardiography and CT (angiography) techniques. It, therefore, offers a comprehensive depiction of the diagnosis and surgical management of cardiovascular diseases.

CONTENTS

Foreword . . . iii
Preface . . . v

The Heart

Introduction . . . 1
The cardiac vessels . . . 2
CT with angiography for the postoperative evaluation of the patency of the grafts . . . 4
Control CT for a triple bypass and reconstructed aortic valve . . . 6
Computed Tomography of both mammary arteries . . . 7
Computed Tomography of a mammary artery and a radial artery as a proximal y-anastomosis. . . . 8
Computed Tomography of off-pump arterial revascularization . . . 9
Computed Tomography of a triple vessel coronary bypass . . . 10
Computed Tomography of a triple vessel coronary bypass . . . 11
Computed Tomography evaluation of a significant case carotid disease . . . 12
Quadruple aorto-coronary bypasses using two arterial and two venous grafts . . . 13
Dextrocardia with triple vessel coronary artery disease . . . 14
Quadruple vessel coronary artery bypass and incidental findings of pulmonary squamous cell carcinoma . . . 16
Myocardial revascularization in the terminal stage of coronary artery disease . . . 18
Coronary artery disease, aneurysm of the left ventricle, valvular disease and aneurysm of the ascending aorta . . . 20
Quintuple vessel coronary bypass with t- graft and jump anastomosis . . . 21
Comparative image of triple vessel coronary disease with selective coronarography and computer angiography . . . 22
Comparative imaging of high stenosis of the right coronary artery by CTA and selective coronarography . . . 23
Right internal mammary artery used with the left radial artery interposed . . . 24
Quadruple vessel coronary bypass using two Y anastomosis and venous grafts. . . . 25
Graft occlusion of the left internal mammary artery . . . 26
An abnormal exit of the left descending branch with stenosis of the circumflex branch . . . 27

Congenital Heart Diseases

Introduction . . . 29
Right coronary ostium agenesis . . . 30
Anomalous Origin of the Left Coronary Artery from the Pulmonary Artery (ALCAPA) syndrome: the Bland-White-Garland syndrome . . . 31
An abnormal inflow of the right pulmonary veins into the inferior vena cava . . . 32
Pulmonary supra-valvular stenosis after complete transposition of the great blood vessels through a combined Rastelli- Lecompte . . . 34

Computed Tomography of congenital heart diseases . . . 36
A left atrial myxoma. . . . 37
Introduction . . . 38

The Aorta

Dissection of the aorta in combination with marfan syndrome . . . 40
Occluded true lumen of the dissected ascending aorta . . . 42
Dissection of the ascending aorta with invagination of the flap into the arch and descending aorta . . . 44
Acute aortic dissection combined with occlusion of the left main artery . . . 46
Ascending aorta dissection with retained rupture. . . . 48
Aortic root aneurysm with chronic dissection of the descending aorta. . . . 50
A thoracic aneurysm following a chronic dissection . . . 52
Prosthesis rupture following an ascending aorta and aortic arch replacement. . . . 54
Aneurysm of the aortic root with aortic valve insufficiency . . . 56
Aneurysm of the aortic root combined with aortic and mitral insufficiency . . . 58
Aneurysm of the aortic root and ascending aorta. . . . 60
Reconstruction of the non-coronary sinus and a replacement of the ascending aorta . . . 62
Aortic root aneurysm with a coarctation of the aorta. . . . 64
Bicuspid aortic valve with an aneurysm of the ascending aorta and the aortic arch . . . 66
An aneurysm of the aortic arch . . . 68
Mycotic aneurysm of the aortic arch and the descending aorta . . . 70
Aneurysm of the descending thoracic aorta. . . . 76
Coarctation of the aorta . . . 78
Surgical treatment of an aortic coarctation . . . 79
Aortic arch aneurysm with infrarenal aorta occlusion . . . 80
Aneurysm of the descending thoracic aorta. . . . 82
Aneurysm of the descending aorta following chronic dissection . . . 84
Ruptured thoraco-abdominal aneurysm with an aorto-oesophageal fistula . . . 86
Aneurysm of the descending aorta following chronic type B dissection . . . 88
A thoracic aneurysm up to the coeliac trunk. . . . 90
A thoracoabdominal aneurysm following acute dissection of the ascending aorta . . . 92
Thoraco-abdominal aneurysm originating from the distal thoracic aorta . . . 94
Thoraco-abdominal aneurysm including the celiac trunk. . . . 96
Ruptured suprarenal aneurysm with chronic occlusion of the mesenteric and the right renal artery. . . . 98
Infrarenal abdomina aneurysm . . . 100
Gigantic infrarenal abdominal aneurysm. . . . 102
Aneurysms of the infrarenal aorta and both internal and external iliac arteries . . . 104
Gigantic aneurysm of the infrarenal aorta and the left iliac artery. . . . 106
An infrarenal aneurysm combined with occlusion of the right superficial femoral artery . . . 108
Occlusion of the infrarenal abdominal aorta . . . 110
Occlusion of the infrarenal aorta and right superfitial femoral artery . . . 112
Occlusion of the infrarenal aorta and both superficial femoral arteries. . . . 114

The Vertebrobasilar Arteries and the Jugular Vein

Introduction . . . 117
Normal blood vessels in the head and neck . . . 118
Stenosis of the left internal carotid artery. . . . 120
Left internal carotid artery bifurcation stenosis and a calcified aortic arch. . . . 122
Left internal carotid artery occlusion . . . 124
Chronic occlusion of the left carotid artery . . . 126
Right internal carotid artery stenosis with a ruptured plaque and a postoperative revision with an autologous vein interposed . . . 128
Acute occlusion of the left common carotid artery with recanalisation and thrombendarteriectomy. . . . 130
Acute occlusion of both internal carotid arteries. . . . 132
In-stent stenosis of the left internal carotid artery. . . . 134

Common carotid artery outflow stenosis with stenosis of the right carotid bifurcation . . . 136
Right carotid artery bifurcation stenosis with chronic occlusion of the left carotid artery . . . 138
Ostial stenosis of the left common and internal carotid artery . . . 140
Stent on the left and thrombendarteriectomy on the right carotid artery . . . 142
Right carotid artery kinking and occlusion of the left internal carotid artery . . . 144
Kinking of both internal carotid arteries . . . 146
Kinking of both internal carotid arteries in a patient with reconstructed aortic valve and replaced ascending aorta . . . 148
Occlusion of the left subclavian and stenosis of the left internal carotid artery . . . 150
Occlusion of the left carotid and the subclavian artery . . . 152
Left subclavian artery occlusion in a patient with coronary artery bypass, using the left internal mammary artery . . . 154
Arterial-venous fistula after jucular punction . . . 156
Aneurysm of the left internal carotid artery . . . 158
Carotid glomus tumour with emphasised kinking of the right carotid artery . . . 160
Tumor of the carotid glomus . . . 162
Vertebral artery stenosis . . . 164
Axillary artery occlusion . . . 166
Ulnar artery occlusion . . . 168
Generalised cardiovascular disease . . . 170
Arteriosclerosis of the distal aorta, combined with carotid disease . . . 172
Stenosis of the left carotid artery and occlusion of the left subclavian artery following aortocoronary bypass grafting . . . 174
Aneurysm on the external jugular vein . . . 176

The Peripheral Blood Vessels

Introduction . . . 179
Computed angiography of lower limbs . . . 181
Right illiac artery occlusion . . . 182
Occlusion of both common illiac arteries . . . 184
Iliac-femoral bypass with an occlusion of the distal superficial femoral artery . . . 186
Efficient femoropopliteal bypass with partial occlusion of the left external iliac artery . . . 188
Occlusion of both iliac arteries . . . 190
Occlusion of the right iliac artery and both superficial femoral arteries . . . 192
Stenosis of the right common femoral artery with occlusion of the right superficial and the left popliteal arteries . . . 194
Occlusion of the iliac, femoral and popliteal arteries following a surgical bypass . . . 196
Occlusion of both superficial femoral arteries . . . 198
Occlusion of both femoral arteries with an occlusion of the right popliteal and crural arteries . . . 200
Occlusion of the left femoral and popliteal arteries with retained flow through the anterior tibial branch . . . 202
Occlusions of the distal femoral and popliteal arteries and the crural branches . . . 204
Combined femoro-crural bypass with a vascular graft and vein . . . 206
Occlusion of the popliteal and crural arteries . . . 208
Popliteal-crural bypass . . . 210
Occlusion of both popliteal arteies . . . 212
Occlusion of the right popliteal artery with an obliterated aneurysm . . . 214
Femoro-fibular bypass with a vascular prosthesis . . . 216
Occlusion of the infrarenal aorta and the left superficial femoral artery . . . 218

The Visceral Arteries

Introduction . . . 221
Aneurysm of the hepatic artery . . . 222
Venous splenic-renal shunt . . . 224

Competing interests and Statements . . . 226
Consent for publication . . . 227
Acknowledgements . . . 228
Biography of Dr Zan Mitrev . . . 229
References . . . 231
Index . . . 235

x

CHAPTER 1

The Heart

Introduction

This chapter introduces the basic anatomy of the human heart and its blood vessels, guided by Computed Tomography (CT) imaging. We present individual case reports describing the surgical management of cardiovascular diseases before and after surgery.

CT coronary arteriography is a non-invasive diagnostic imaging modality with an intravenously administered iodine contrast medium that allows visualisation of the origin and course of the coronary arteries, assess stenosis, bypass grafts, aneurysm(s) and to evaluate atherosclerotic plaque formation [1, 2].

The resultant volumetric dataset is interpreted using primary transverse reconstructions as well as multiplanar reformations, and 3D volume-rendering reconstructions which provide a selective visualisation of the anatomic relationships among vessels and surrounding osseous structures.

Unenhanced ECG-synchronized cardiac CT is indicated for detecting and quantifying coronary artery calcium: "calcium scoring" [3].

Main categories of CT-based analyses and indications are:

1. Evaluation of coronary arteries for atherosclerosis or anomalies
2. Assessment of non-coronary pathology including great vessels, chambers, myocardium, valves, or pericardium
3. Estimation of cardiac chamber function, including ejection fraction and chambers volumes
4. Morbidity risk determination of patients presenting with symptoms of stable angina or acute chest pain
5. Discordant or inconclusive stress tests

The cardiac vessels

3D Volume rendering (VR) images of the left anterior descending artery (LAD), the circumflex artery (CX) **(Fig. 1-1)**, the right coronary artery **(Fig. 1-2)** and the topo-anatomical 3D-image of the coronary arteries in correlation with the left ventricle **(Fig. 1-3)** are shown.

The heart is supplied with oxygenated blood via two main blood vessels, the left main coronary artery (LMN) and the right coronary artery (RCA); they originate at the base of the ascending aorta just above the aortic valve: the coronary ostia [4, 5]. The anatomy of the heart blood vessels is shown in **Figure 1-4 to 1-7**. A CT with coronary angiography allows a postoperative evaluation of the patency of the grafts; **Figure 1-8** shows 3D images of surgical revascularization of the myocardium with grafts of the left internal mammary artery (LIMA) on the left anterior descending artery (LAD), grafted using the left radial artery (LRA) on the first diagonal branch (Dg1) and the saphenous vein graft on the circumflex artery (LCx). **Figure 1-9** displays a CT preview of the grafts.

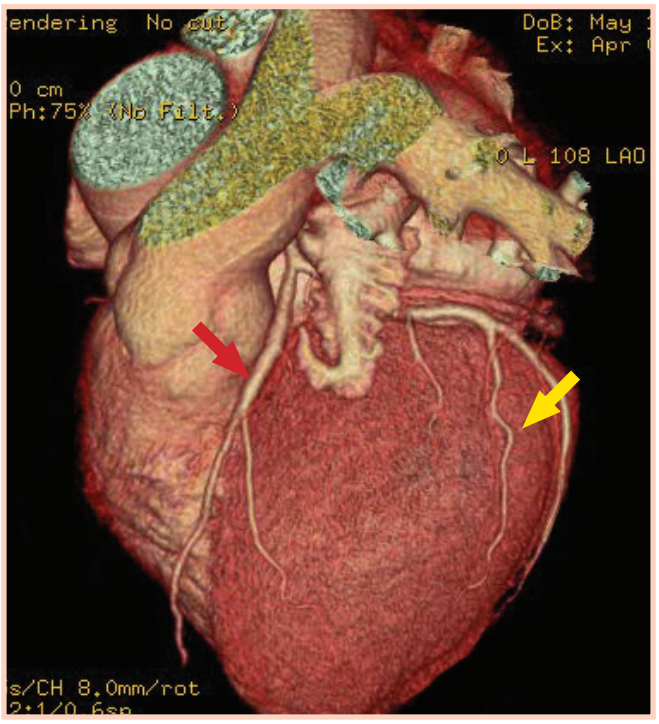

Fig. 1-1: 3D VR Image of the left anterior descending artery (LAD) *(red arrow)* and artery (CX) *(yellow arrow)*.

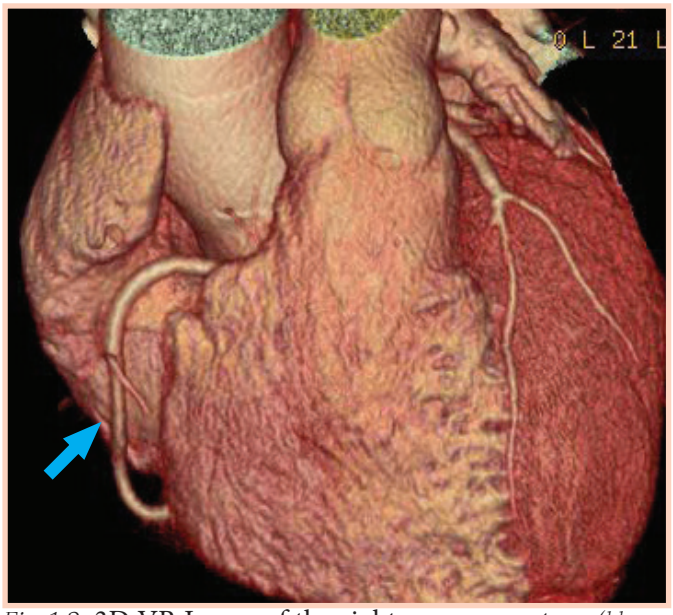

Fig. 1-2: 3D VR Image of the right coronary artery *(blue arrow)*.

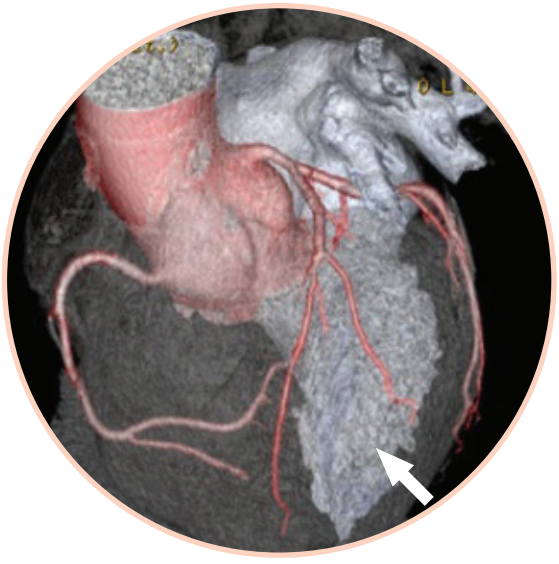

Fig. 1-3: 3D VR Topo-anatomical three-dimensional image of the coronary arteries in correlation with the left ventricle *(white arrow)*.

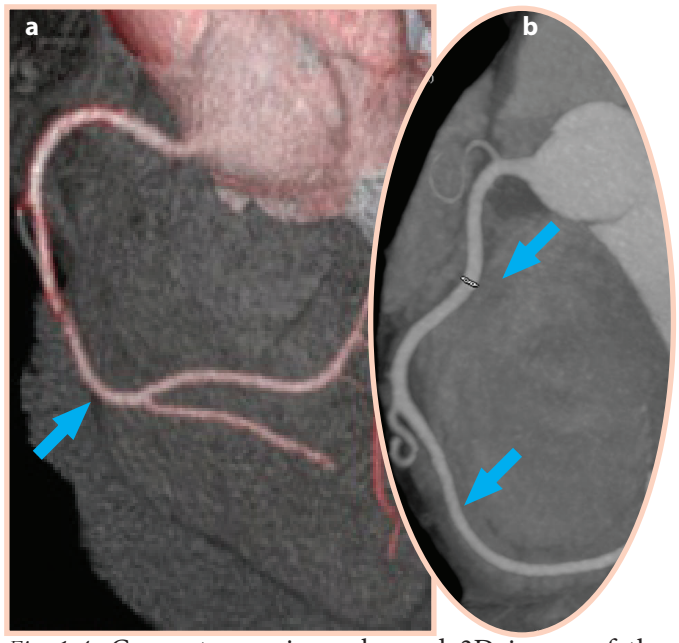

Fig. 1-4: Computer angiography and 3D image of the right coronary artery (a and b, RCA) *(blue arrow)*.

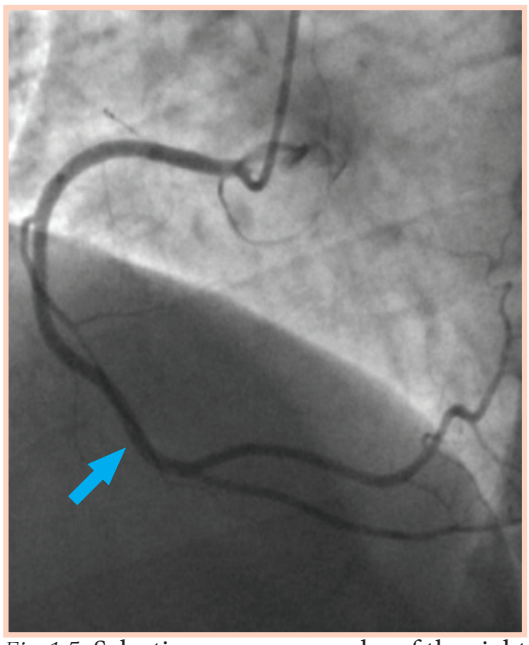

Fig. 1-5: Selective coronarography of the right coronary artery (RCA) *(blue arrow)*.

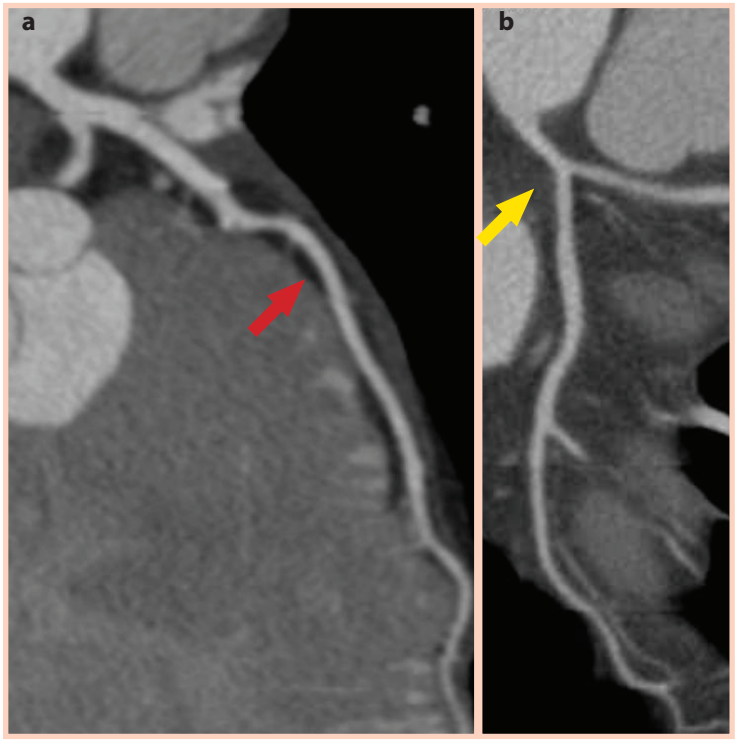

Fig. 1-6: CT image of the left anterior descending artery (LAD) *(a, red arrow)* and the left circumflex artery(LCx) *(b, yellow arrow)*.

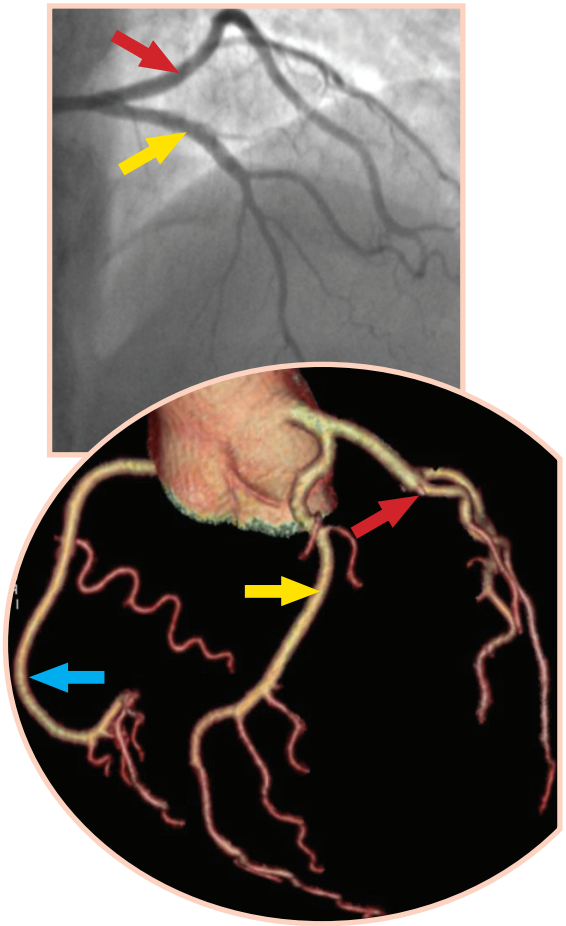

Fig. 1-7: A comparative image of selective coronarography (upper image) and computer 3D VR image (lower image) of the coronary arteries: LAD *(red arrow)*, LCx *(yellow arrow)* and RCA *(blue arrow)*.

CT with angiography for the postoperative evaluation of the patency of the grafts

A 3D Image of surgical re-vascularisation of the myocardium with grafts of the left internal mammary artery (LIMA) on the left anterior descending artery (LAD), grafted using the left radial artery (LRA) on the first diagonal branch (Dg1) and the saphenous vein graft (VSG) on the circumflex artery (LCx) is shown in **Figure 1-8**. **Figure 1-9** shows a CT preview of the grafts of LIMA on LAD, LRA on RD1 and VSG on RCX.

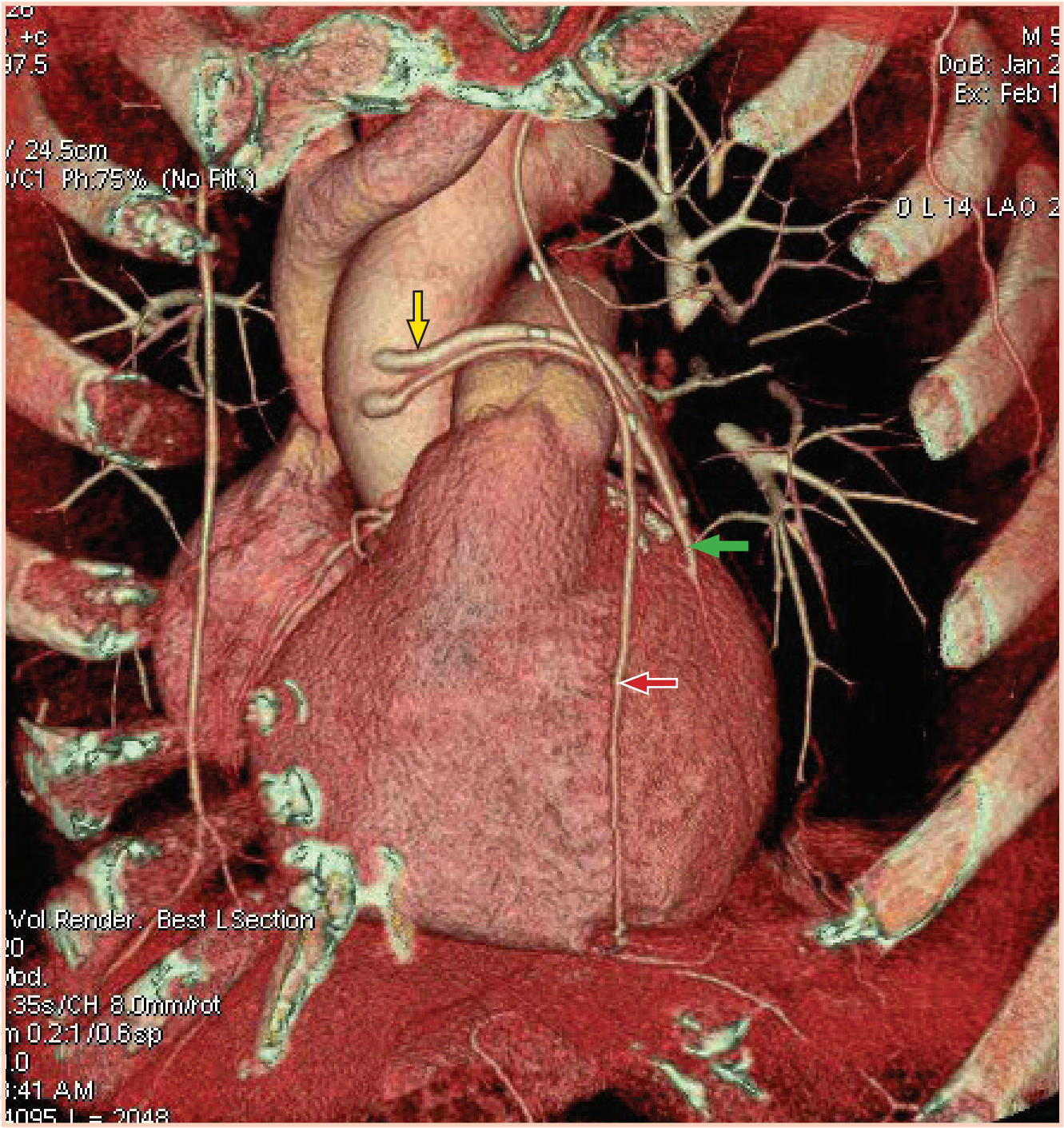

Fig. 1-8: 3D Image of surgical re-vascularisation of the myocardium with grafts of the left internal mammary artery (LIMA) on the left anterior descending artery (LAD) *(red arrow)*, grafted using the left radial artery (LRA) on the first diagonal branch (Dg1) *(green arrow)* and the saphenous vein graft on the circumflex artery (LCx) *(yellow arrow)*.

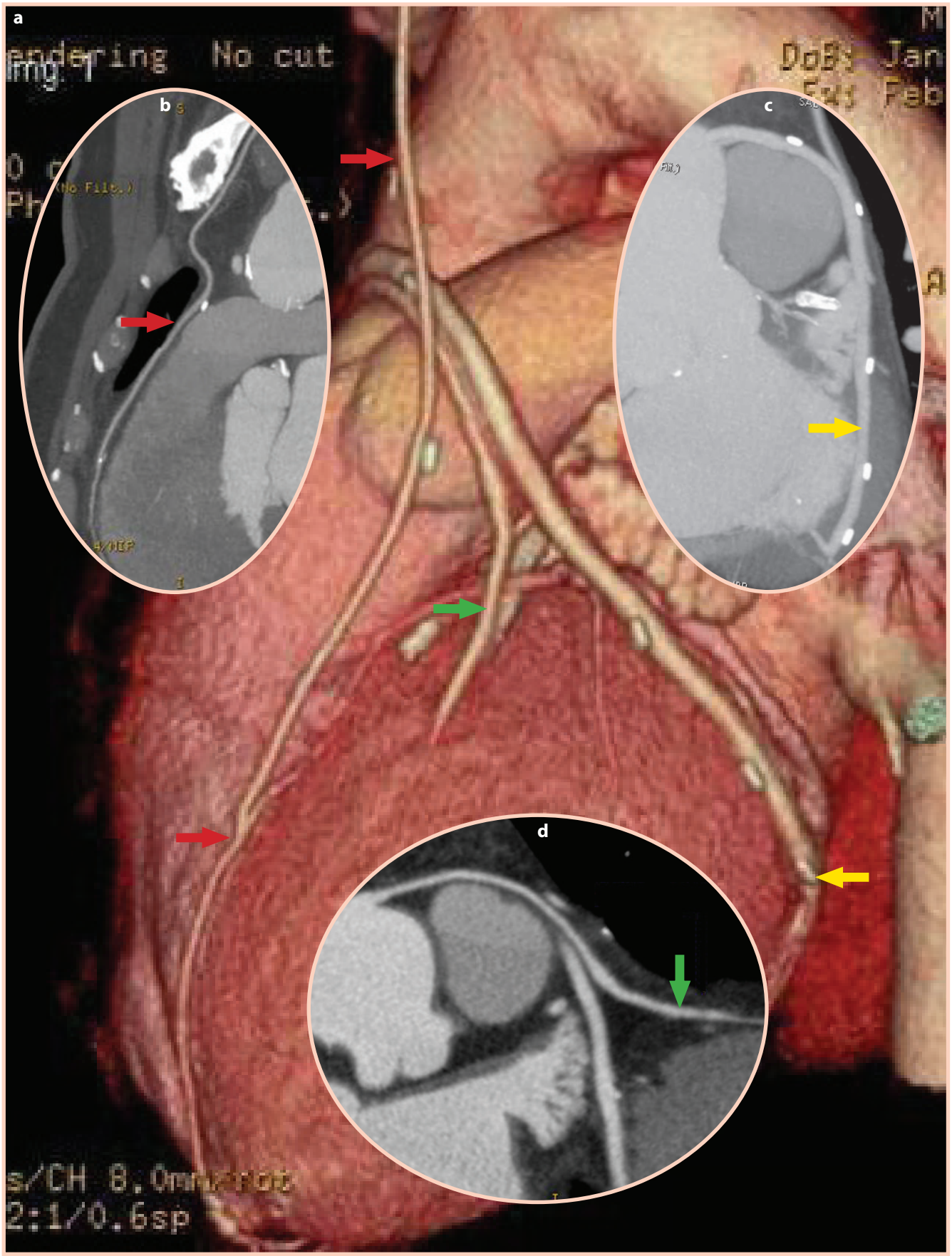

Fig. 1-9: CT preview of the grafts of LIMA on LAD (a and b, red arrow), LRA on RD1 *(a, green arrow)* and Venous graft on LCX *(c, yellow arrow)*.

Control CT for a triple bypass and reconstructed aortic valve

T. N., a 75-year-old patient was surgically treated in 2002 with triple bypass grafting. One year later, he had a reconstruction of the aortic valve due to severe aortic valve stenosis. Ten years later, he developed symptomatic mitral valve stenosis.

As a preoperative evaluation for mitral valve surgery, CT was performed, where normal graft patency as well as the normal morphology and functionality of the aortic valve were confirmed **(Figs. 1-10 and 1-11)**.

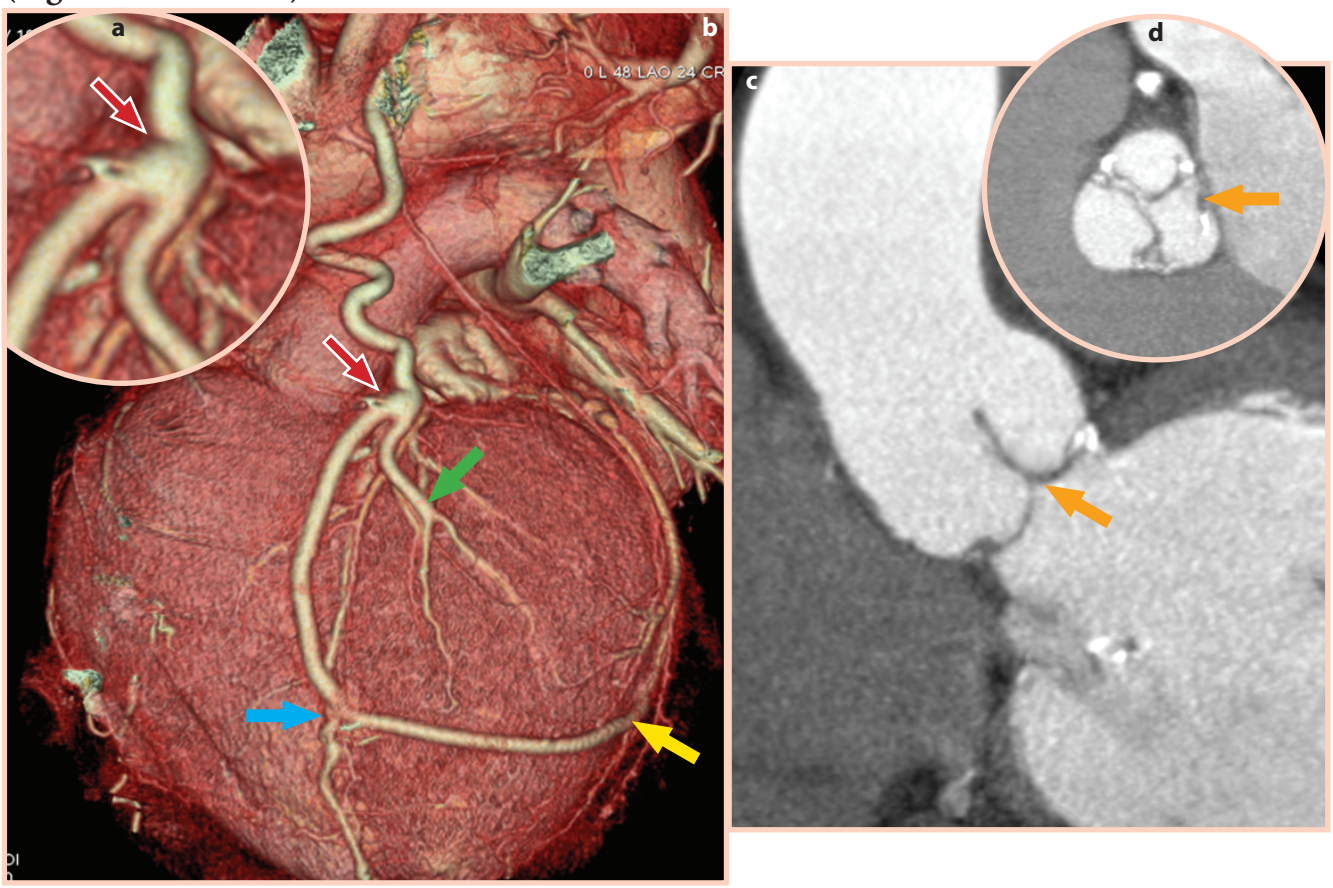

Fig. 1-10: CT image of distal anastomosis on the left internal mammary artery (LIMA) with the first diagonal branch *(b, green arrow)* as well as proximal anastomosis with the left radial artery as a Y anastomosis on LIMA (a, b, red arrow) that continues as a "jump" anastomosis to LAD *(b, blue arrow)* and to the marginal branch *(b, yellow arrow)*. The reconstructed aortic valve is shown(with three handcrafted pericardial leaflets) (c, d, orange arrow).

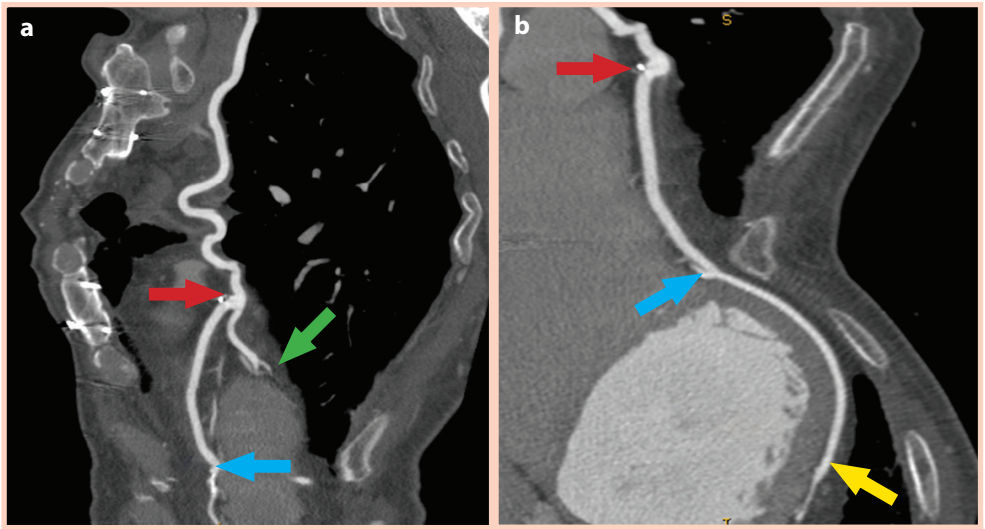

Fig. 1-11: CT image of Y anastomosis of LIMA on proximal LAD/Dg1 (a, b, red arrow), LIMA on Dg1 *(a, green arrow)*, LRA with a jump to distal LAD (a, b, blue arrow) and LRA to CX *(b, yellow arrow)*.

Computed Tomography of both mammary arteries

K. L., a 66-year-old patient, had a triple bypass done 7 years previously, despite complaints of unspecific chest pain; the CT showed adequate patency of the grafts **(Figs. 1-12 and 1-13)**.

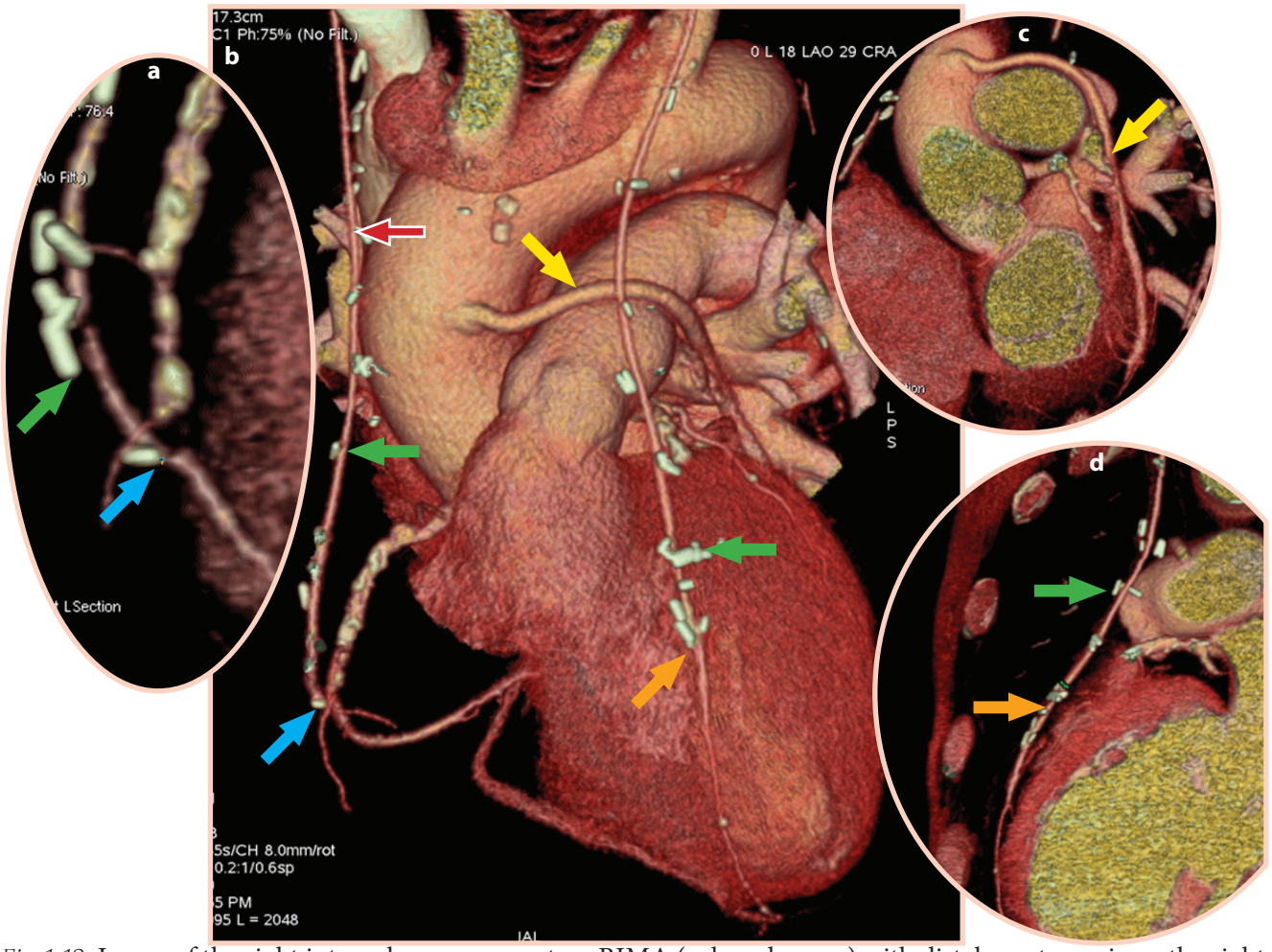

Fig. 1-12: Image of the right internal mammary artery RIMA (a, b, red arrow) with distal anastomosis on the right coronary artery (RCA) (a, b, blue arrow), vein graft to the left circumflex artery (LCx) (b, c, yellow arrow) and the left internal mammary artery (LIMA) with the left descending artery (LAD) (b, d, orange arrow). Clips on LIMA and RIMA *(green arrow)*.

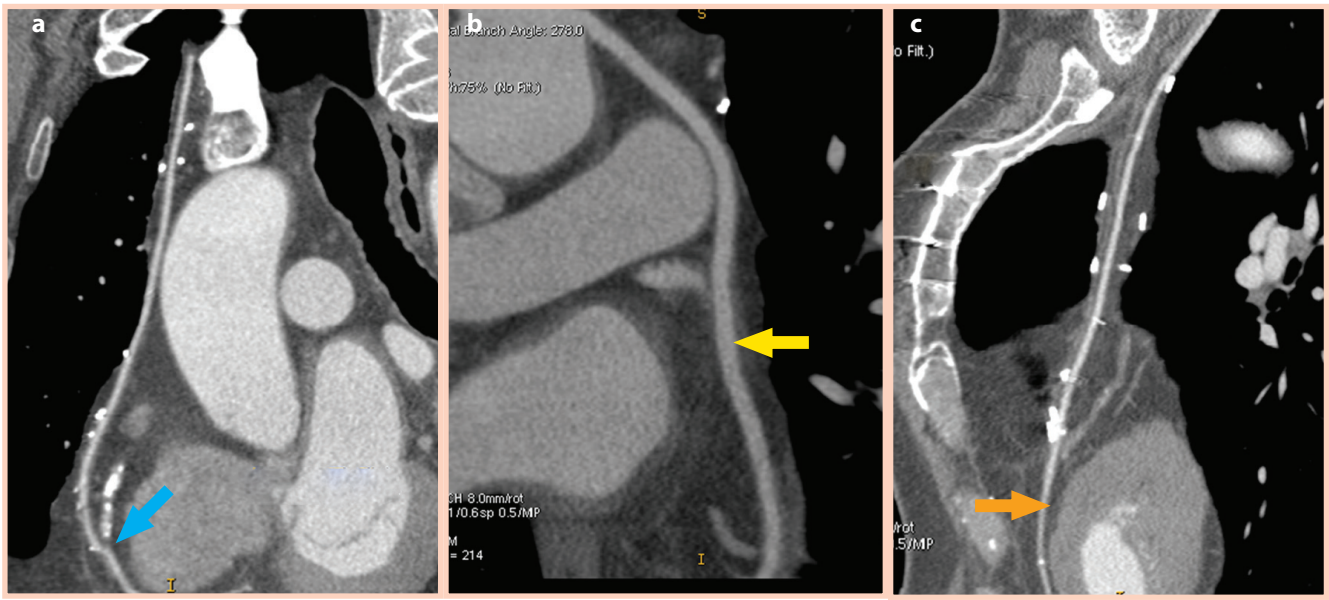

Fig. 1-13: CT of patent grafts of RIMA on RCA *(a, blue arrow)*, venous graft on LCx *(b, yellow arrow)* and LIMA on LAD *(c, orange arrow)*.

Computed Tomography of a mammary artery and a radial artery as a proximal y-anastomosis

Z. N., a 79-year-old patient, who had undergone surgical revascularization of the myocardium 7 years previously, using double arterial bypass grafts, was admitted due to heavy breathing, chest pain, coughing and fatigue. Computed imaging for diagnostic purposes was performed. The 3D imaging of patent through the arterial grafts, with a proximal Y anastomosis of the left radial artery (LRA) with the left internal mammary artery (LIMA) that passes to the right coronary artery (RCA) and LIMA to the left anterior descending artery (LAD), is presented in **Figure 1-14**. The image of the patency through the distal anastomosis of LRA with RCA is shown in **Figure 1-15**, while the image of the patent through the distal anastomosis of LIMA on LAD is shown in **Figure 1-16**.

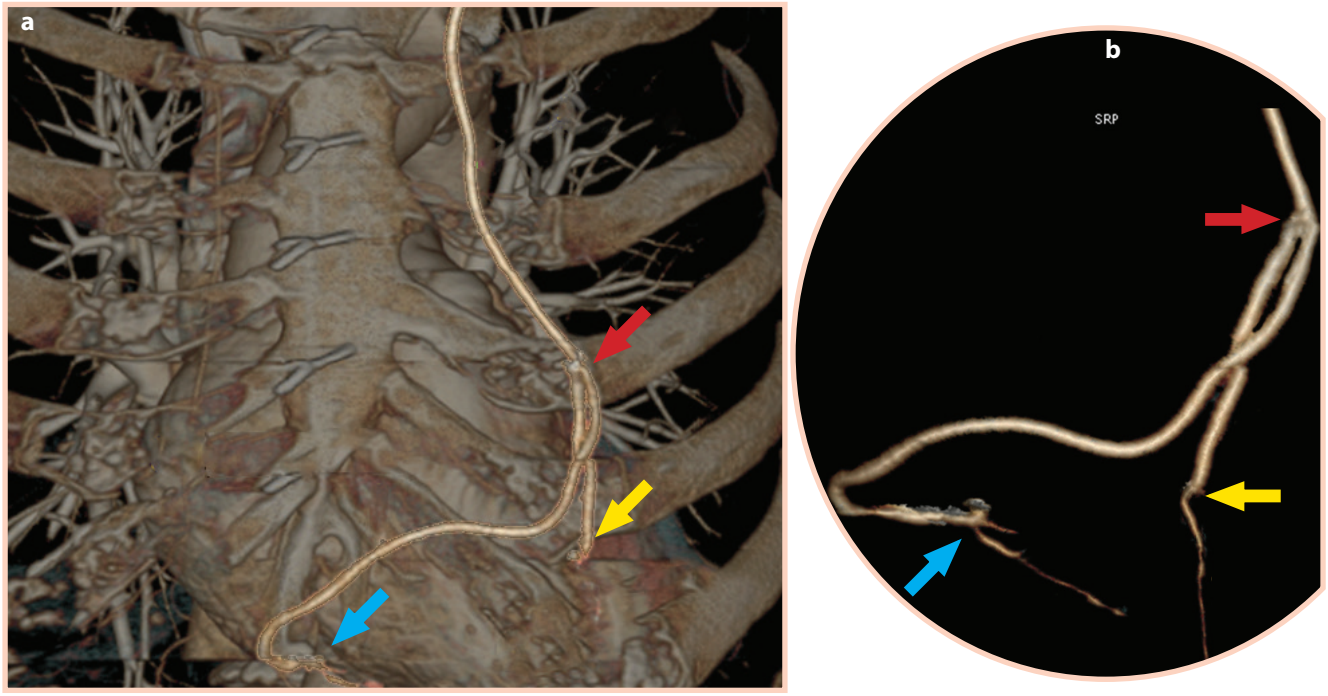

Fig. 1-14: 3D imaging of patency through the arterial grafts with a proximal Y anastomosis of the left radial artery (LRA), with the left internal mammary artery (LIMA) *(red arrow)* that passes to the right coronary artery (RCA) *(blue arrow)* and LIMA to the left anterior descending artery (LAD) *(yellow arrow)*.

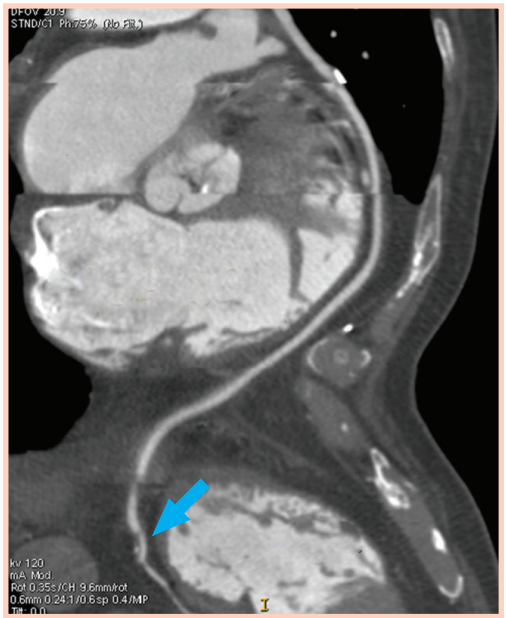

Fig. 1-15: Curved image of patent through the distal anastomosis of LRA with RCA *(blue arrow)*.

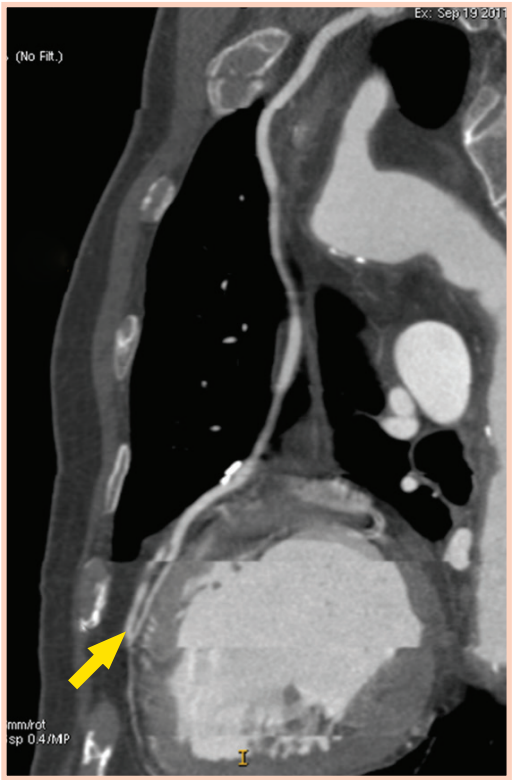

Fig. 1-16: Image of patent through the distal anastomosis of LIMA on LAD *(yellow arrow)*.

Computed Tomography of off-pump arterial revascularization

E. I., a 63-year-old patient, had a double aortocoronary bypass grafted on a beating heart (OP-CAB technique) 8 years previously. He was admitted due to unspecific angina symptoms and a CT was performed **(Fig. 1-17)**.

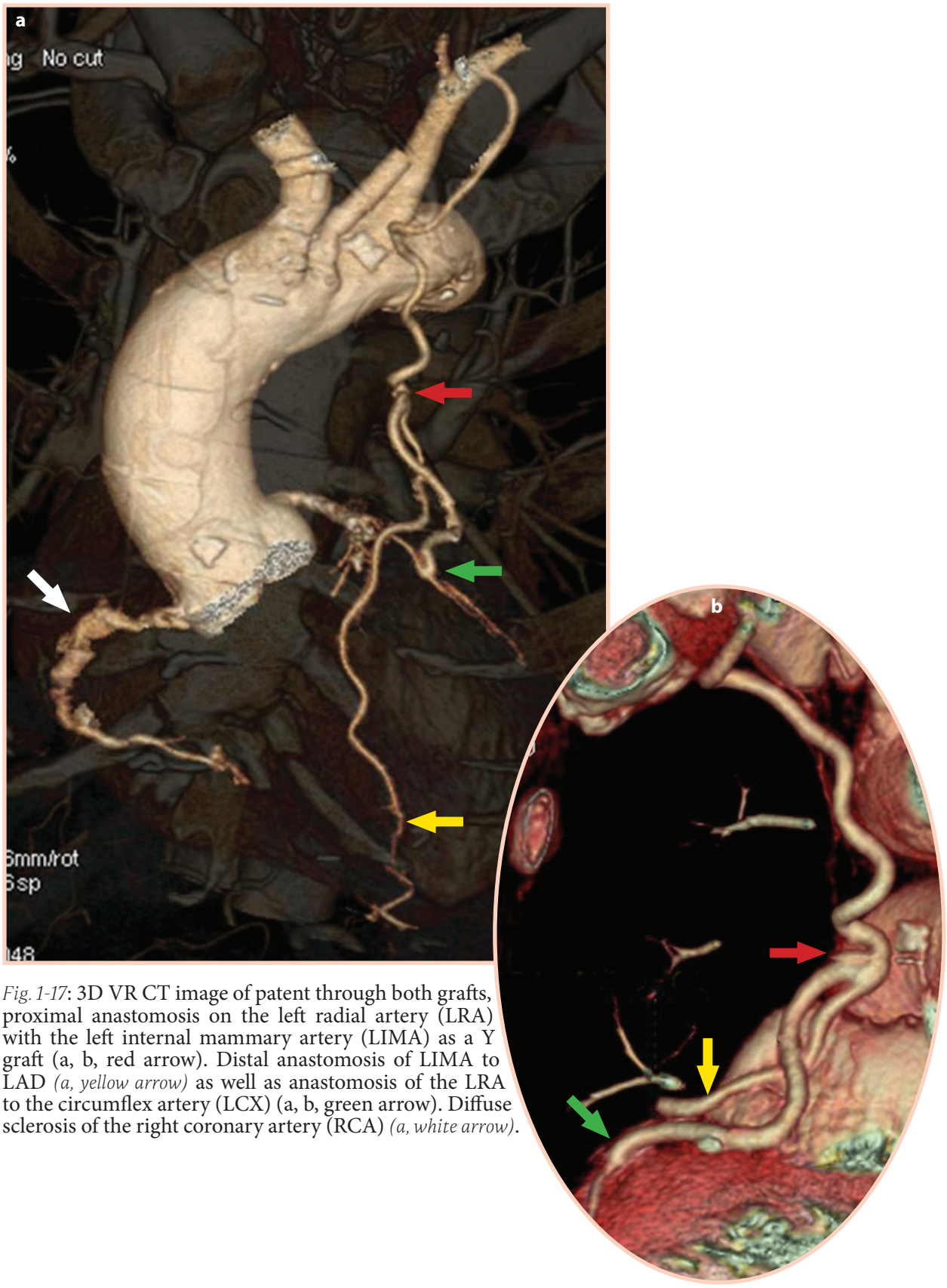

Fig. 1-17: 3D VR CT image of patent through both grafts, proximal anastomosis on the left radial artery (LRA) with the left internal mammary artery (LIMA) as a Y graft (a, b, red arrow). Distal anastomosis of LIMA to LAD *(a, yellow arrow)* as well as anastomosis of the LRA to the circumflex artery (LCX) (a, b, green arrow). Diffuse sclerosis of the right coronary artery (RCA) *(a, white arrow)*.

Computed Tomography of a triple vessel coronary bypass

R. D., a 71-year-old patient subjected to a triple vessel aortocoronary bypass grafting 7 years previously, was admitted due to unspecific angina-like symptoms. The CT showed no patency in the grafts **(Figs. 1-18 and 1-19)**.

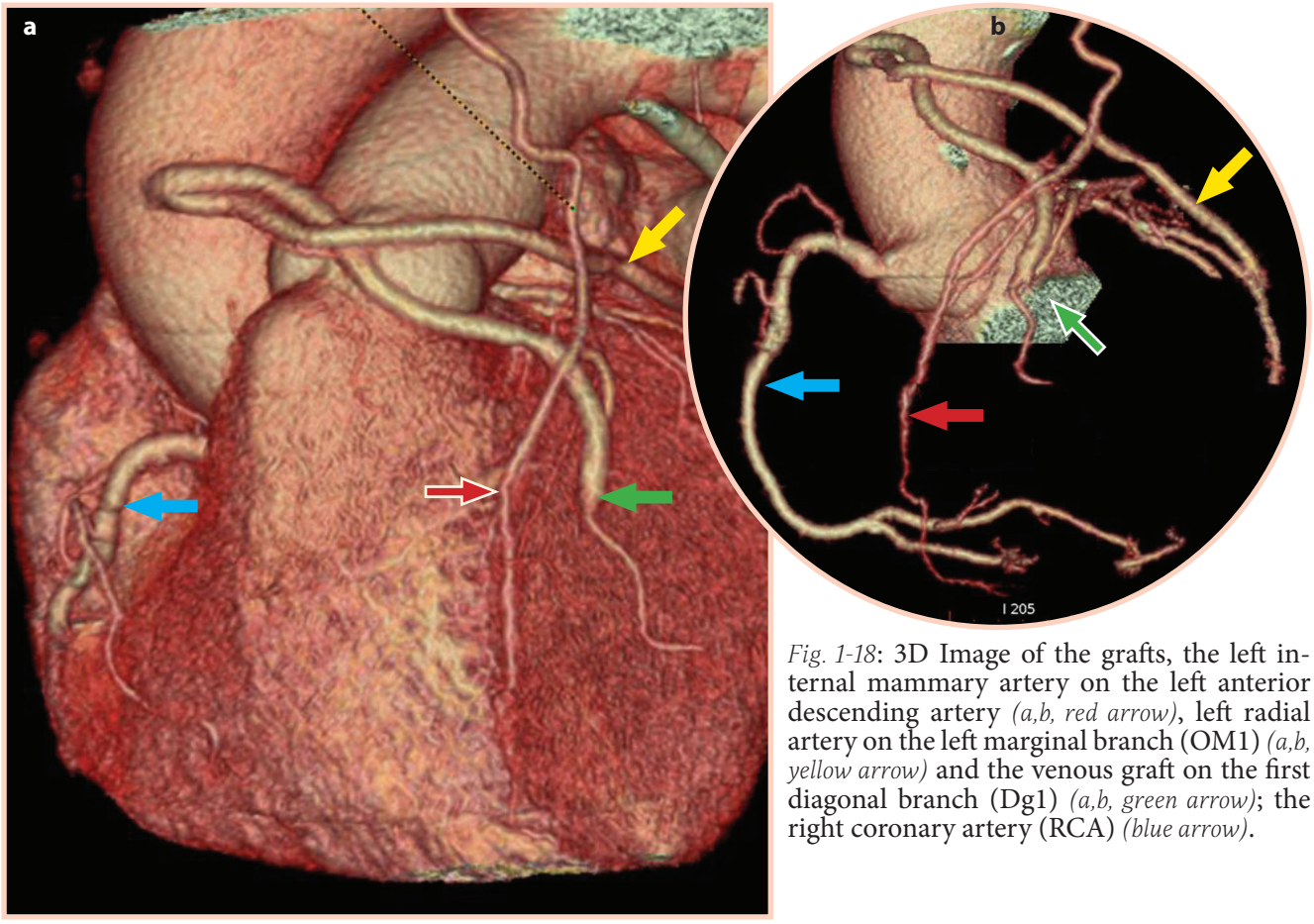

Fig. 1-18: 3D Image of the grafts, the left internal mammary artery on the left anterior descending artery *(a,b, red arrow)*, left radial artery on the left marginal branch (OM1) *(a,b, yellow arrow)* and the venous graft on the first diagonal branch (Dg1) *(a,b, green arrow)*; the right coronary artery (RCA) *(blue arrow)*.

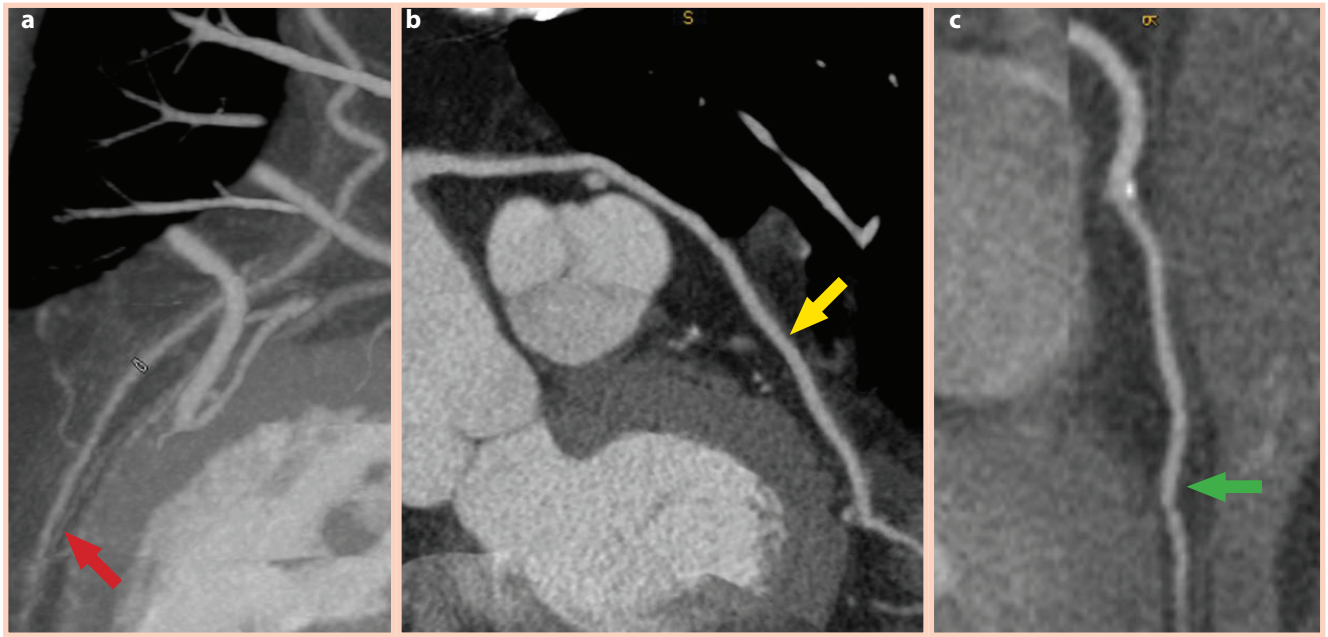

Fig. 1-19: CT angiography of adequately placed grafts, LIMA on LAD *(a, red arrow)*, LRA on OM1 *(b, yellow arrow)* and con Rd1 *(c, green arrow)*.

Computed Tomography of a triple vessel coronary bypass

O. G., a 68-year-old patient who had a quintuple vessel coronary revascularization six months before, complained of unspecified chest pain. The CT showed normal graft patency **(Fig. 1-20)**.

Fig. 1-20: 3D image of normal flow through the grafts, distal anastomosis of the left internal mammary artery (LIMA) to the left anterior descending artery (LAD) *(red arrow)*, segment of the left radial artery as a Y graft with LIMA *(yellow arrow)* and distally to the first diagonal branch Dg1 *(green arrow)*, free graft of LRA on the first marginal branch (OM1) *(white arrow)*, venous graft to OM2 *(orange arrow)* and Venous graft to the right coronary artery (RCA) *(blue arrow)*.

Computed Tomography evaluation of a significant case carotid disease

M. H., a 62-year-old patient, had a double aortocoronary bypass 8 months previously and was admitted following syncopal episodes. On the CT, patent through the graft was seen, but also high stenosis of the right internal carotid artery (ACI) was verified **(Fig. 1-21)**. Surgical thromb-endarteriectomy on the right ACI was performed **(Figs. 1-22 and 1-23)**.

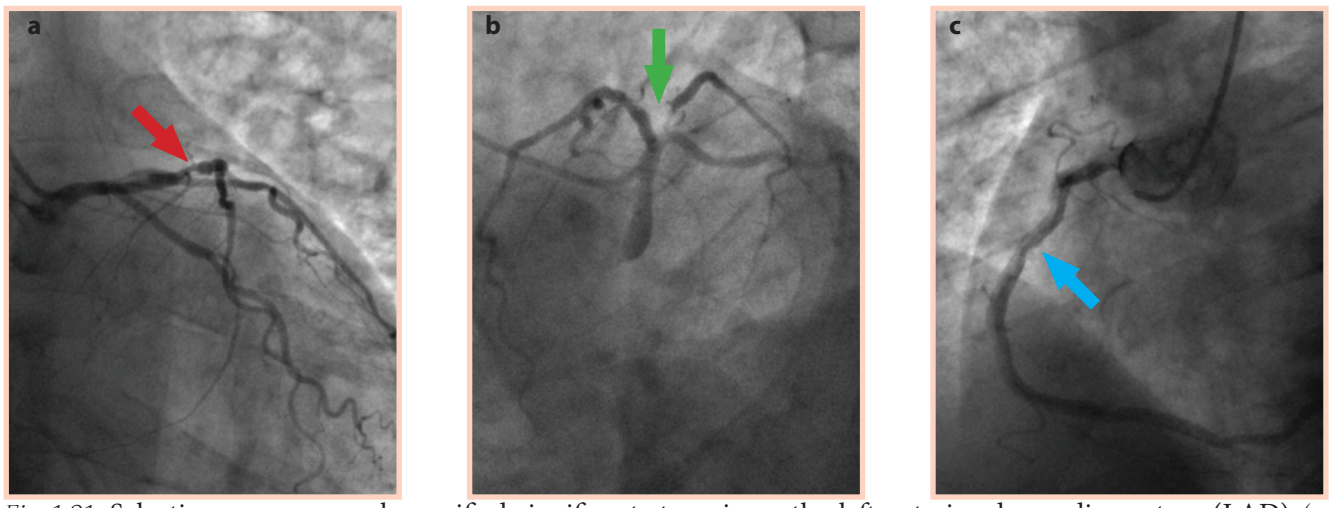

Fig. 1-21: Selective coronarography verified significant stenosis on the left anterior descending artery (LAD) *(a, red arrow)*, occlusion of the first marginal branch (OM1) *(b, green arrow)* and non-significant stenosis of the right coronary artery (RCA) *(c, blue arrow)*.

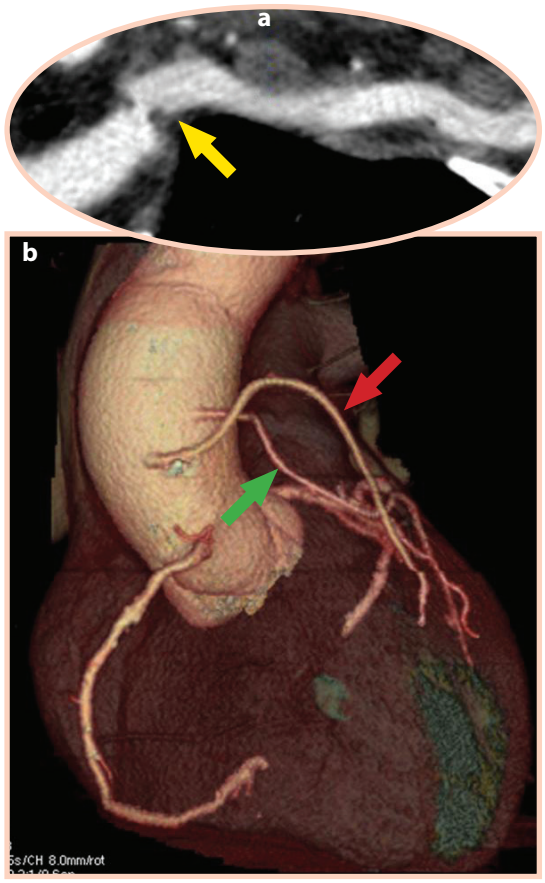

Fig. 1-22: A 3D image of patent through the left internal mammary artery (LIMA) *(b, red arrow)*. as a free graft on the LAD, the left radial artery (LRA) as a free graft of the intermediate branch (Rim) *(b, green arrow)*. High stenosis of the left subclavian artery *(a, yellow arrow)*.

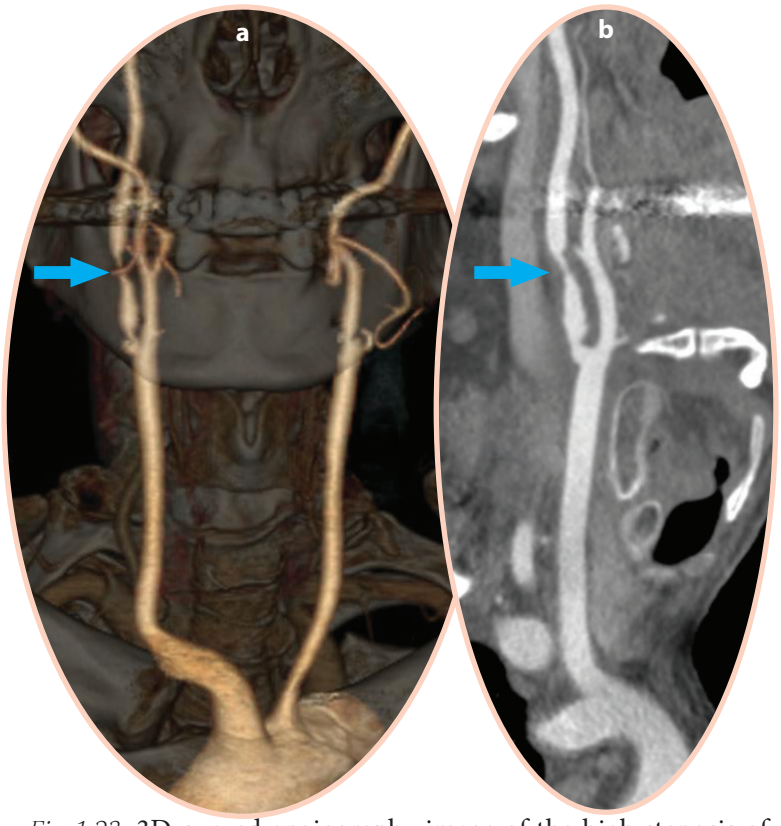

Fig. 1-23: 3D curved angiography image of the high stenosis of the right internal carotid artery (ACI dex) (a, b, blue arrow).

Quadruple aorto-coronary bypasses using two arterial and two venous grafts

I. I., a 65-year-old patient, complained of abnormal chest pain following bypass surgery. At 3-months follow-up, CT was performed. **Figure 1-24** shows the 3D image of the grafts of the left internal mammary artery (LIMA) to the left anterior descending artery (LAD), the venous graft (VSG) for the first diagonal artery (Dg1), the left radial artery (LRA) as a free graft to the circumflex artery (Cx) and the venous graft on the right coronary artery (RCA). The CT angiography images of the distal anastomosis of LIMA on LAD, VSG on RCA, LRA on Cx and venous graft on Dg1 are shown in **Figure 1-25**.

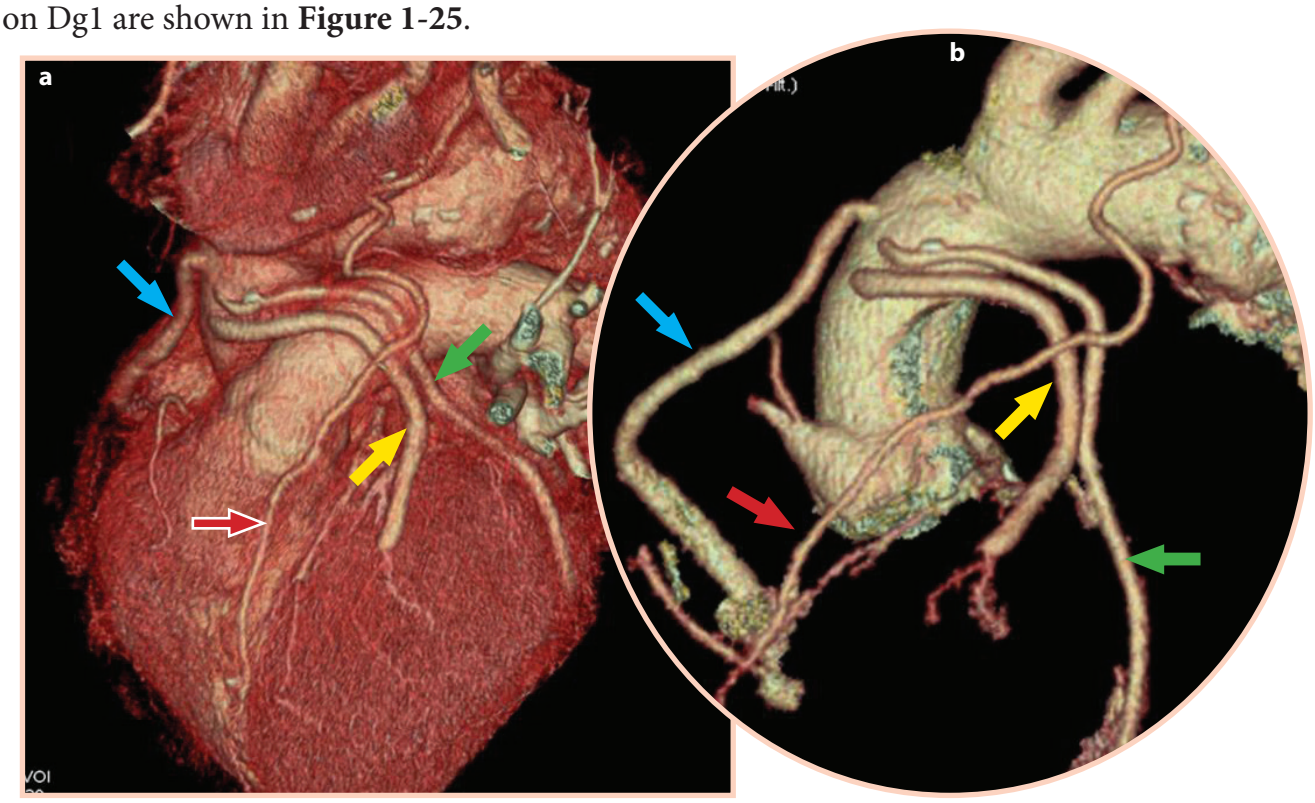

Fig. 1-24: 3D image of the grafts of the left internal mammary artery (LIMA) to the left anterior descending artery (LAD) *(red arrow)*, the venous graft for the first diagonal artery (Dg1) *(yellow arrow)*, the left radial artery (LRA) as a free graft to the circumflex artery (Cx) *(green arrow)* and the venous graft on the right coronary artery (RCA) *(blue arrow)*.

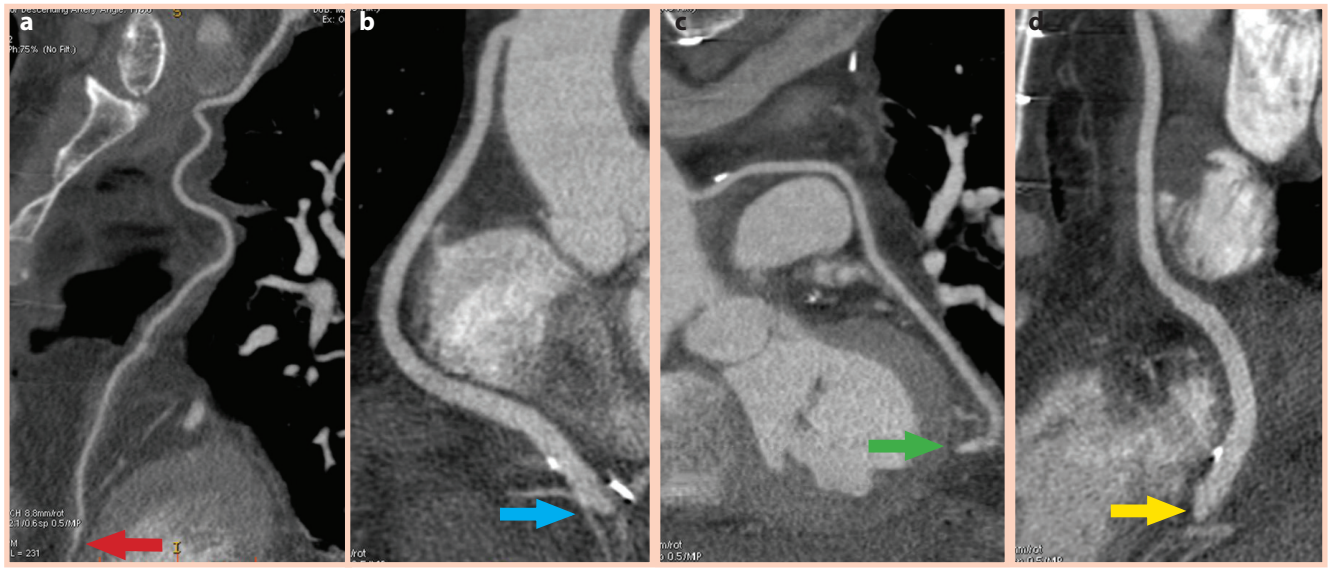

Fig. 1-25: CT angiography imaging of the distal anastomosis of LIMA on LAD *(a, red arrow)*, venous graft on RCA *(b, blue arrow)*, LRA on Cx *(c, green arrow)*, venous graft on Dg1 *(d, yellow arrow)*.

Dextrocardia with triple vessel coronary artery disease

M. S., a 49-year-old patient with a history of myocardial infarction and heart failure symptoms, dyspnoea and angina that had intensified in the previous 3 months, was admitted to the hospital. Using selective coronarography, a triple vessel coronary artery disease and situs inversus totalis. Postoperative CT was performed **(Figs. 1-26, 1-27 and 1-28)**.

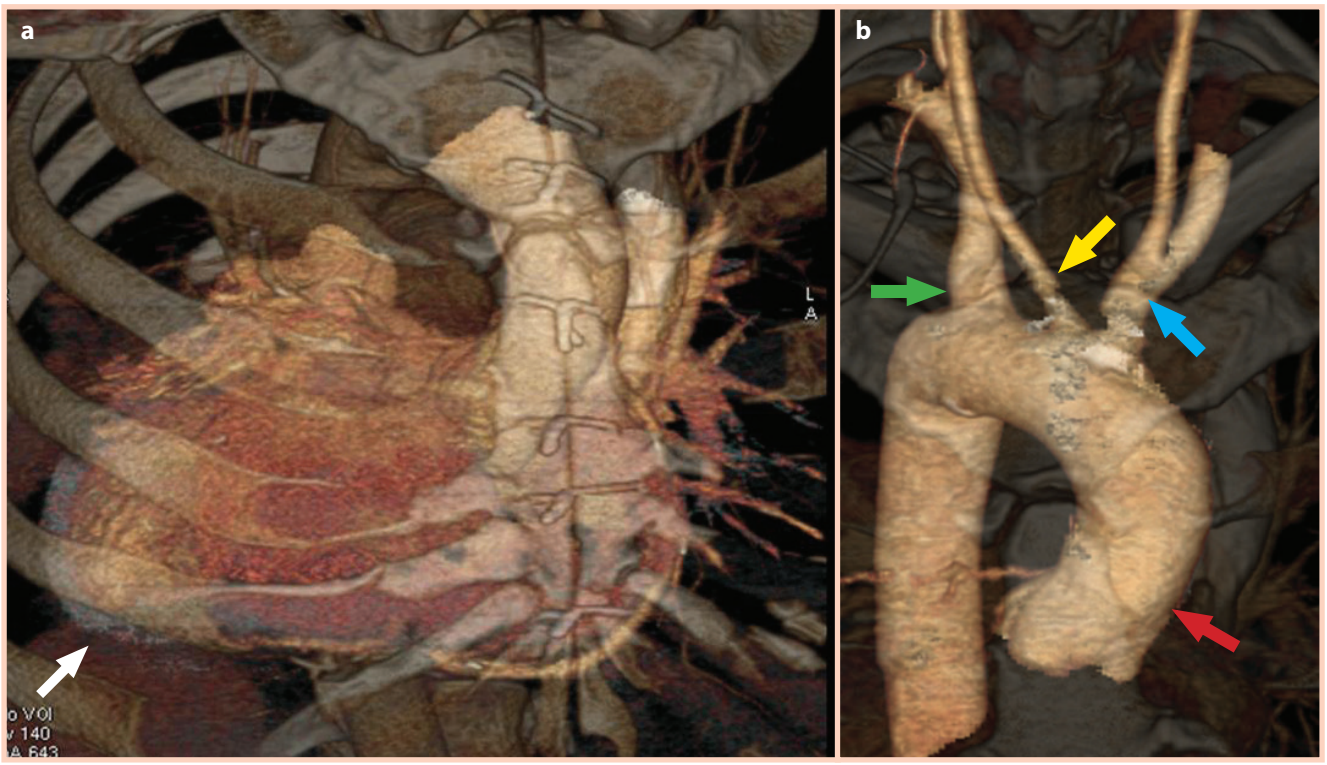

Fig. 1-26: Topo-anatomical 3D image of situs inversus totalis with dextrocardia. Left ventricle completely positioned on the right side of the chest *(a, white arrow)*. Image of the right positioned ascending aorta *(b, red arrow)*, brachiocephalic branch with right carotid *(b, blue arrow)*, left carotid *(b, yellow arrow)* and right subclavian artery *(b, green arrow)*.

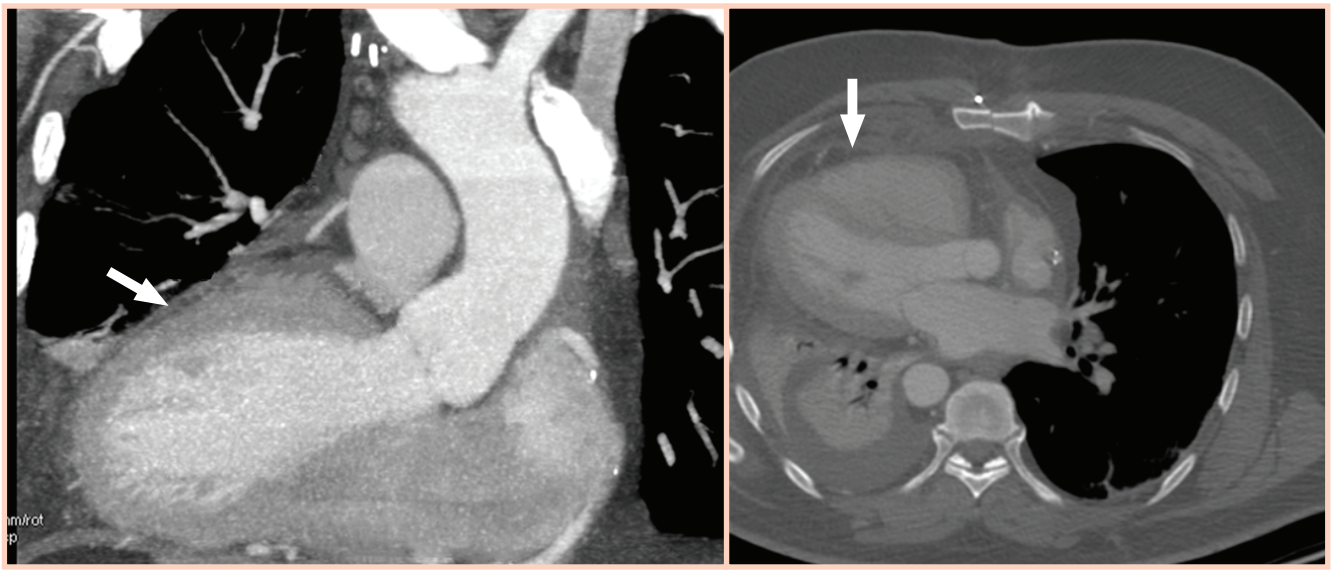

Fig. 1-27: CT image of the left ventricle positioned on the right side of the chest *(white arrow)*.

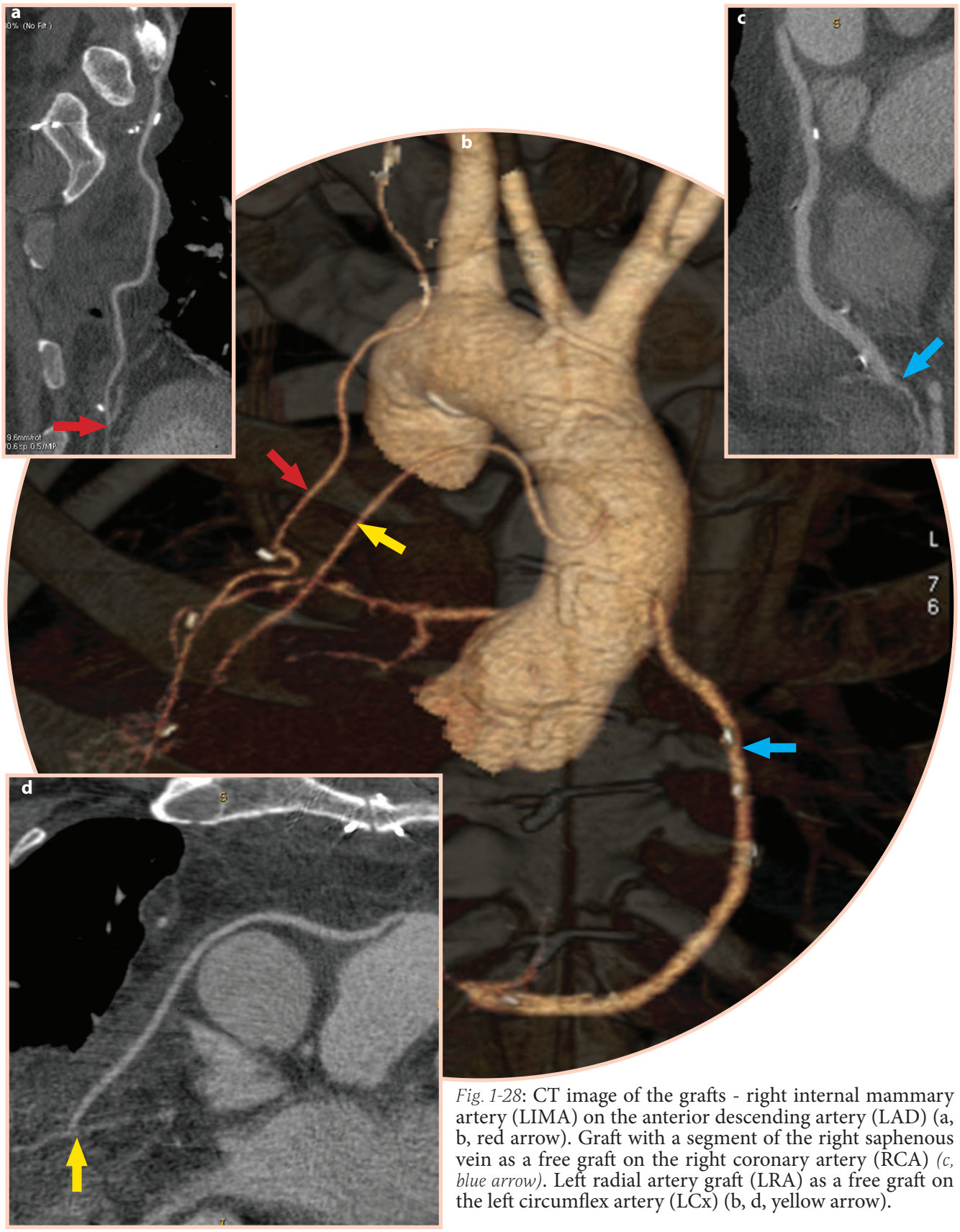

Fig. 1-28: CT image of the grafts - right internal mammary artery (LIMA) on the anterior descending artery (LAD) (a, b, red arrow). Graft with a segment of the right saphenous vein as a free graft on the right coronary artery (RCA) *(c, blue arrow)*. Left radial artery graft (LRA) as a free graft on the left circumflex artery (LCx) (b, d, yellow arrow).